

See discussions, stats, and author profiles for this publication at: <https://www.researchgate.net/publication/231175203>

# Intramolecular Photochemical Electron Transfer. 2. Fluorescence Studies of Linked Porphyrin- Quinone Compounds

ARTICLE *in* JOURNAL OF THE AMERICAN CHEMICAL SOCIETY · NOVEMBER 1983

Impact Factor: 12.11 · DOI: 10.1021/ja00363a002

---

CITATIONS

110

---

READS

17

7 AUTHORS, INCLUDING:



Aleksander Siemiarczuk

Photon Technology International, Inc.

46 PUBLICATIONS 1,609 CITATIONS

SEE PROFILE



James R Bolton

University of Alberta

314 PUBLICATIONS 9,440 CITATIONS

SEE PROFILE

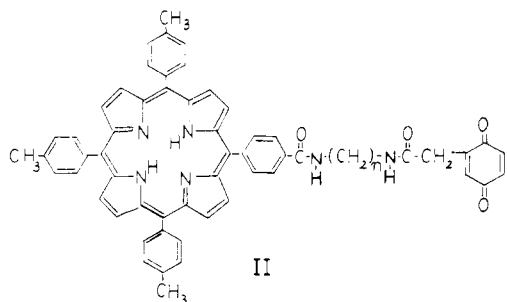
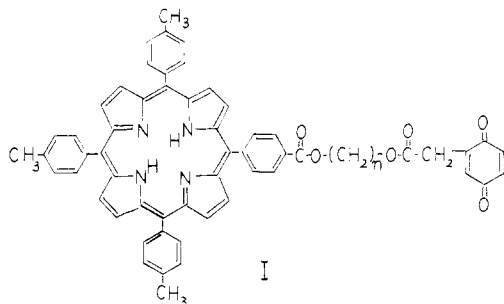
## Intramolecular Photochemical Electron Transfer. 2. Fluorescence Studies of Linked Porphyrin-Quinone Compounds<sup>1a</sup>

Aleksander Siemiarz, <sup>†1b,2</sup> Alan R. McIntosh, <sup>†1b</sup> Te-Fu Ho, <sup>†1b</sup> Martin J. Stillman, <sup>\*†3</sup> Kenneth J. Roach, <sup>†1b</sup> Alan C. Weedon, <sup>\*†1b</sup> James R. Bolton, <sup>\*†1b</sup> and John S. Connolly <sup>\*†</sup>

Contribution from the Photochemistry Unit, Department of Chemistry, The University of Western Ontario, London, Ontario, Canada N6A 5B7, and the Photoconversion Research Branch, Solar Energy Research Institute, Golden, Colorado 80401. Received March 28, 1983

**Abstract:** Systematic studies of absorption spectra and fluorescence spectra and lifetimes have been carried out on a series of *meso*-tetratolylporphyrins to which various molecular entities have been covalently attached via diamide linkages with the two amides being separated by *n* methylene groups (*n* = 2, 3, or 4). The attached end groups include *p*-benzoquinone, hydroquinone, and dimethoxybenzene. These studies reveal the existence of at least two more or less distinct forms: a family of "complexed" conformers in which the end group is likely folded so as to interact with the porphyrin, and one or more "extended" conformers in which the porphyrin moiety is relatively unperturbed by the end group. The complexed conformers exhibit perturbations of spectra and diminished fluorescence lifetimes and quantum yields as compared with the extended conformer(s). Oxidation of the porphyrin-linked hydroquinone form to the quinone form does not significantly affect the absorption or fluorescence spectra but causes strong quenching of fluorescence and diminution of the fluorescence lifetimes. This quenching is interpreted primarily in terms of electron transfer from the lowest excited singlet state of the porphyrin to the quinone moiety. On the basis of the assumption that these shorter fluorescence lifetimes of the quinone relative to the hydroquinone are due entirely to electron transfer, apparent electron-transfer rate constants *k*<sup>et</sup> at room temperature range from  $<1 \times 10^8$  to  $>7 \times 10^9$  s<sup>-1</sup>, depending on solvent and probably the specific geometry of the conformers. Quenching in both sets of conformers appears to be thermally activated and is strongly inhibited in frozen matrices. Parallel studies of porphyrin-quinone molecules with various methylene chains (*n* = 2, 3, and 4) indicate that the geometry of the linkage is critical to the rate of electron transfer. A methylene chain with *n* = 3 appears to be optimum.

In paper 1 of this series<sup>4</sup> we described EPR and optical spectroscopic evidence that demonstrated that visible light can induce a stabilized intramolecular charge separation in a series of diamide-linked porphyrin-quinones (II) with a quantum yield as



high as 2–3% in moderately polar frozen solvents at low temperatures. We also demonstrated that the product of the photochemical reaction is a biradical ion pair consisting of a porphyrin

cation radical and a quinone anion radical ( $P^+ \cdot Q^-$ ). In an earlier communication<sup>5</sup> we had demonstrated a similar stabilized intramolecular electron transfer in an analogous series of diester-linked porphyrin-quinones (I). These molecules were synthesized according to the procedure of Kong and Loach,<sup>6</sup> who have also observed stable EPR signals by visible-light irradiation of I and its zinc derivatives.<sup>7</sup>

Molecules such as I and II and other porphyrin-quinone (PQ) linked molecules,<sup>8</sup> have been proposed as models for the reaction-center protein of photosynthesis. Indeed, in most of these molecules photochemical electron transfer appears to occur from the excited singlet state, since fluorescence is strongly quenched as compared with porphyrins without a quinone attached. It is known that the primary photochemical electron-transfer reaction in both photosystems I and II of green-plant and algal photo-

(1) (a) Contribution No. 300 from the Photochemistry Unit, Department of Chemistry, The University of Western Ontario. (b) Photochemistry Unit, University of Western Ontario.

(2) Permanent address: Institute of Physical Chemistry, Polish Academy of Sciences, Warsaw, Poland.

(3) Centre for Interdisciplinary Studies in Chemical Physics, University of Western Ontario.

(4) McIntosh, A. R.; Siemiarz, A.; Bolton, J. R.; Stillman, M. J.; Ho, T.-F.; Weedon, A. C. *J. Am. Chem. Soc.*, preceding paper in this issue.

(5) Ho, T.-F.; McIntosh, A. R.; Bolton, J. R. *Nature (London)* **1980**, *286*, 254–256.

(6) Kong, J. L. Y.; Loach, P. A. *J. Heterocycl. Chem.* **1980**, *17*, 737–744.

(7) (a) Kong, J. L. Y.; Spears, K. G.; Loach, P. A. *Photochem. Photobiol.* **1982**, *35*, 545–553. (b) Loach, P. A.; Runquist, J. A.; Kong, J. L. Y.; Dannhauser, T. J.; Spears, K. G. In "Electrochemical and Spectrochemical Studies of Biological Redox Components", Kadish, K. M., Ed.; American Chemical Society, Washington, DC, 1982; ACS Symp. Ser. No. 201, pp 515–561.

(8) (a) Nishitani, S.; Kurata, N.; Sakata, Y.; Misumi, S.; Migita, M.; Okada, T.; Mataga, N. *Tetrahedron Lett.* **1981**, *22*, 2099–2102. (b) Migita, M.; Okada, T.; Mataga, N.; Nishitani, S.; Kurata, N.; Sakata, Y.; Misumi, S. *Chem. Phys. Lett.* **1981**, *84*, 263–266. (c) Netzel, T. L.; Bergkamp, M. A.; Chang, C.-K.; Dalton, J. *J. Photochem.* **1981**, *17*, 451–460. (d) Bergkamp, M. A.; Dalton, J.; Netzel, T. L. *J. Am. Chem. Soc.* **1982**, *104*, 253–259. (e) Tabushi, I.; Koga, N.; Yanagita, M. *Tetrahedron Lett.* **1979**, No. 3, 257–260. (f) Harriman, A.; Hosie, R. J. *J. Photochem.* **1981**, *15*, 163–167. (g) Ganesh, K. N.; Sanders, J. K. M. *J. Chem. Soc., Chem. Commun.* **1980**, 1129–1131.

<sup>†</sup> The University of Western Ontario.

<sup>‡</sup> Solar Energy Research Institute.

synthesis occurs out of an excited singlet state of chlorophyll.<sup>9</sup>

Very little is known about the structural requirements for, or indeed the precise mechanism of, intramolecular electron transfer in these synthetic systems. Fluorescence properties are an important probe; however, aside from some preliminary observations, the fluorescence spectra and lifetimes of these molecules have not previously been characterized systematically. This is the subject of this paper.

### Experimental Section

The compounds utilized in this study were 5-(4-carboxyphenyl)-10,15,20-tritylporphyrin (TTPa), 5-(4-(*N*-propylcarbamoyl)phenyl)-10,15,20-tritylporphyrin (PAPr), the linked porphyrin-quinone compounds II (PAnAQ, where *n* is the number of methylene groups in the bridge), and the corresponding hydroquinone [PAnA(QH<sub>2</sub>)] and dimethoxybenzene [PAnA(DMB)] derivatives of II. PAPr was synthesized by Roach (unpublished) while the other compounds were synthesized by Ho et al. as described elsewhere.<sup>10</sup>

UV-visible absorption spectra were obtained with 1.00-cm cuvettes in either a Hewlett-Packard Model 8450A or a Cary Model 219 spectrophotometer. Steady-state fluorescence spectral measurements were carried out on Perkin-Elmer Model MPF-4 or Spex Fluorolog spectrofluorimeters.

Fluorescence-lifetime measurements were conducted on a Photochemical Research Associates Model 3000 nanosecond lifetime fluorometer<sup>11</sup> by the method of time-correlated single-photon counting.<sup>12</sup> A pulsed hydrogen-arc lamp was used as the excitation source; the full-width-at-half-maximum (fwhm) of the pulse was ~1–4 ns when the lamp was operated at ~30 kHz.

Because of the low fluorescence yields, coupled with emission in the red to near-IR region, fluorescence count rates were low when monochromators were used in both emission and excitation beams. Connolly et al.<sup>13</sup> have discussed in considerable detail the problems of measuring fluorescence lifetimes under these conditions. In most experiments broad-band detection was employed by removing the emission monochromator and replacing it with a Corning CS 2-58 (640 nm) cut-off filter. The advantage of this arrangement, in addition to the higher count rates, is that the emission represents the populations of all the excited states in the sample, limited only by the extent to which photoselection is accomplished by the choice of excitation wavelength. The disadvantage is that, in the case of PQ molecules, deconvolution of the emission profiles into a finite ( $\leq 3$ ) number of single-exponential components was not always possible. Accordingly, in other experiments the emission monochromator was replaced with one equipped with a near-IR grating. With the techniques described by Connolly et al.<sup>13b</sup> and slits at a bandwidth of 16 nm, it was possible to obtain reproducible data within a reasonable time period ( $\leq 10$  h) while having the capability to vary both the emission and excitation wavelengths. Some additional experiments were conducted with picosecond laser excitation (~5–10 ps fwhm, 590 nm) coupled with time-correlated single-photon counting as described by Ware and co-workers.<sup>14</sup> The half-width of the instrument response function of this instrument was ~20 ps.

Room-temperature fluorescence lifetime measurements were carried out with a nonthermostated sample holder with square 1.00-cm fluorescence cuvettes. Some low-temperature experiments were conducted with a cylindrical Pyrex tube (8 mm o.d.) inserted into a quartz dewar mounted in place of the room-temperature sample holder. Temperatures were regulated by varying the flow rate of N<sub>2</sub> gas passing through a dewar filled with liquid nitrogen and then through the quartz dewar; temperatures were measured directly in the sample tube by means of a calibrated copper-constantan thermocouple. Additional experiments were conducted with an Air Products Displex closed-cycle helium cryostat, which provided continuously variable temperatures over the range of interest. In these experiments, a special heavy-walled 1.00-cm-

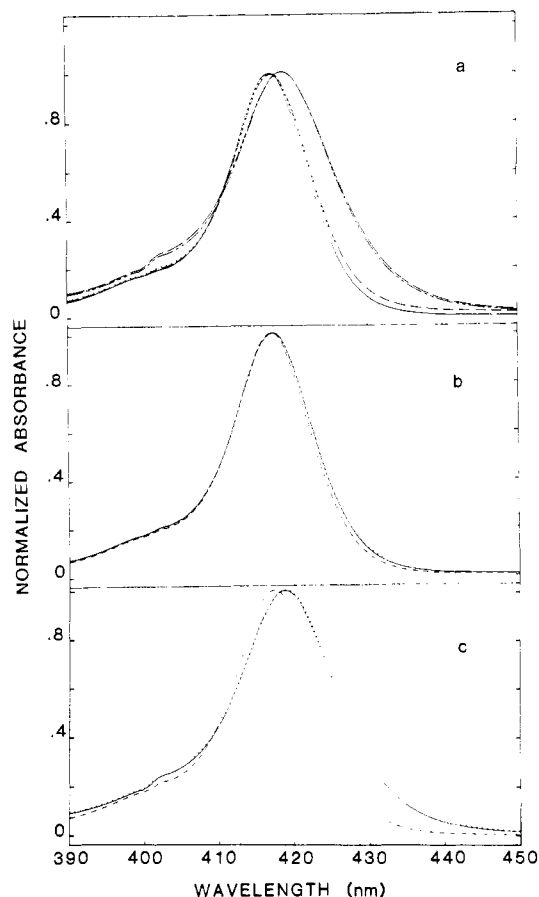


**Figure 1.** Absorption spectra at room temperature in CH<sub>2</sub>Cl<sub>2</sub> measured in the Soret region. Spectra were normalized at the maximum of the Soret band to emphasize the differences among them. (a) TTPa (—); PAPr (···); PA3A(DMB) (---); II (*n* = 3) (untreated) (-·-·-); II (*n* = 3) oxidized with PbO<sub>2</sub> (----). (b) PA2A(DMB) (—); PA3A(DMB) (---). (c) II (untreated): *n* = 2 (—); *n* = 3 (···); *n* = 4 (---).

square Suprasil cuvette was placed in the cryostat housing, and emission was collected at a 90° angle with respect to the excitation beam. Temperatures were measured with an auxiliary, calibrated copper-constantan thermocouple placed in the vicinity of the sample, while the output of the main (gold-chromel) thermocouple was coupled in a feed-back circuit to an internal heating element to maintain temperatures at  $\pm 0.5$  K.

Sample concentrations used were typically  $10^{-5}$  to  $10^{-6}$  M; fluorescence lifetimes were found to be independent of concentration over the range  $10^{-4}$  to  $10^{-7}$  M. Samples were deaerated by bubbling with prepurified nitrogen or argon gas for 10–15 min. All solvents were of spectroscopic grade or were distilled and checked for fluorescence under experimental conditions. 2-Methyltetrahydrofuran (mTHF) was taken either from freshly distilled solvent or from a stock stored at 77 K after fractional distillation to remove peroxides and the BHT inhibitor.

Fluorescence lifetimes were obtained by computer deconvolution of each decay profile against the respective lamp profile obtained at the excitation wavelength, usually in the Soret band of the porphyrin. This method has been thoroughly tested by Connolly et al.<sup>13</sup> and proved to give highly reproducible fluorescence lifetimes for chlorophyll *a* and bacteriochlorophyll *a*; in these studies there was also a large gap between the excitation and emission wavelengths. The  $\chi^2$  test and the appearance of random residuals at the 95% confidence level were used as criteria for goodness of fit.<sup>11–13</sup>

Oxidation of the hydroquinone form of the linked PQ compounds and determination of the degree of oxidation to the quinone form were carried out by procedures outlined in paper 1.<sup>4</sup> Briefly, UV absorption spectra of unlinked methyl-*p*-benzoquinone and its corresponding hydroquinone were used to determine the proportion of the two forms of II in the various samples. Untreated II (*n* = 2, 3, or 4) was found by these methods to be a mixture of about 25:75 PAnAQ and PAnA(QH<sub>2</sub>).

Reduction of untreated II to PAnA(QH<sub>2</sub>) was attempted with NaBH<sub>4</sub> in a number of solvents. However, the resulting absorption spectra indicated that in no case could a clean, stoichiometric reduction be obtained. Hence, no fluorescence measurements were carried out on fully reduced samples of II.

(9) Katz, J. J.; Norris, J. R.; Shipman, L. L.; Thurnauer, M. C.; Wasielewski, M. R. *Annu. Rev. Biophys. Bioeng.* **1978**, *7*, 393–434.

(10) Ho, T.-F.; McIntosh, A. R.; Weedon, A. C. *Can. J. Chem.*, submitted for publication.

(11) Gudgin, E.; Lopez-Delgado, R.; Ware, W. R. *Can. J. Chem.* **1981**, *59*, 1037–1044.

(12) Ware, W. R. In "Creation and Detection of the Excited State"; Ware, W. R., Ed.; Marcel Dekker: New York, 1971; Vol. I, pp 213–301.

(13) (a) Connolly, J. S.; Janzen, A. F.; Samuel, E. B. *Photochem. Photobiol.* **1982**, *36*, 559–563. (b) Connolly, J. S.; Samuel, E. B.; Janzen, A. F. *Ibid.* **1982**, *36*, 565–574.

(14) Ware, W. R.; Pratinidi, M.; Bauer, R. K. *Rev. Sci. Instrum.* **1983**, in press.

(15) Seybold, P. G.; Gouterman, M. *J. Mol. Spectrosc.* **1969**, *31*, 1–13.

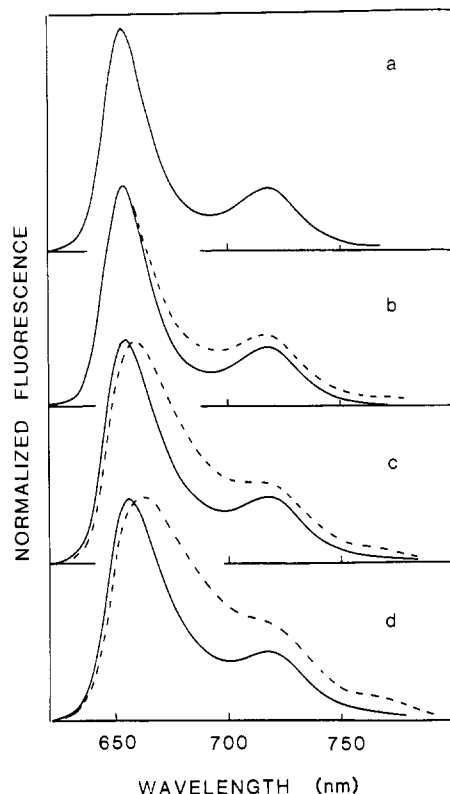


Figure 2. Normalized fluorescence spectra (uncorrected) obtained in  $\text{CH}_2\text{Cl}_2$  at room temperature ( $\text{N}_2$ -saturated) with excitation wavelengths 420 nm (—) and 440 nm (---). (a) TTPa or PAPr. (b) PA3A(DMB). (c) II ( $n = 3$ ) (untreated). (d) II oxidized with  $\text{PbO}_2$  to PA3AQ.

## Results and Discussion

**1. Spectroscopic and Photophysical Properties of II and Some Model Compounds. a. Absorption Spectra.** Absorption spectra in the Soret region of the various porphyrins studied are shown in Figure 1. The spectra of PAPr and PA4A(DMB) are very similar to that of TTPa, exhibiting only very slight broadening in the order  $\text{TTPa} < \text{PA4A(DMB)} < \text{PAPr} < \text{PA2A(DMB)} < \text{PA3A(DMB)}$ . In contrast, both II ( $n = 2$ ) and II ( $n = 3$ ) exhibit Soret bands that are considerably broader and red-shifted compared to TTPa. The length of the methylene chain has a strong effect on the spectra of II but has only a minor influence on the spectra of the corresponding dimethoxy derivatives. We interpret these spectral differences as being due to the formation of intramolecular complexes in which the aryl moiety at the end of the diamide chain folds in such a way as to interact with the  $\pi$ -electron system of the porphyrin macrocycle. Thus, it appears that the broadening of the Soret band of II ( $n = 2$  and 3) may be due to a close proximity of the two chromophores. The much diminished effect in the dimethoxybenzene derivatives (see Figure 1b) is probably due to steric effects of the methoxy groups, which prevent a close approach. These folding interactions appear to be negligible in II ( $n = 4$ ) since in this case the spectrum is practically identical with that of PA4A(DMB).

Oxidation of untreated II ( $n = 3$ ) to >95% PA3AQ has only a very slight narrowing effect on the Soret band (see Figure 1a). Thus it appears that oxidation of the hydroquinone form of PQ to the corresponding quinone has little effect on the spectral line broadening.

**b. Fluorescence Spectra and Quantum Yields.** The fluorescence spectra of TTPa and PAPr are identical and are independent of the excitation wavelength in the Soret region (Figure 2a). However, the fluorescence spectra of the linked porphyrins are generally broader and red-shifted compared to the unlinked porphyrins, especially when excited at the long-wavelength edge of the Soret band (compare the solid and dashed curves in Figure 2b–2d). The broadening and red shifts of the emission spectra observed when the molecules are excited in the region of the

Table I. Estimated Fluorescence Quantum Yields ( $\phi_f$ ) in  $\text{CH}_2\text{Cl}_2$  at Room Temperature Relative to TPP<sup>a</sup>

compd	$\phi_f^b$ ( $\lambda_{\text{ex}}$ , nm)	$\phi_f^b$ ( $\lambda_{\text{ex}}$ , nm)
TTPa	0.13 (420)	
PA3A(DMB)	0.11 (420)	
PAPr	0.11 (420)	
II ( $n = 3$ )	0.053 (418)	0.033 (430)
(untreated) <sup>c</sup>		0.015 (440)
II ( $n = 3$ )	0.021 (410)	0.012 (440)
(oxidized) <sup>d</sup>	0.025 (418)	

<sup>a</sup>  $T = 295 \text{ K}$ ;  $\text{N}_2$  saturated. <sup>b</sup> Measured from integrated intensities relative to *meso*-tetraphenylporphyrin (TPP) assumed to have a fluorescence quantum yield of 0.11 in aerated benzene.<sup>15</sup> Excitation wavelengths are shown in parentheses. All values are  $\pm 10\%$ . <sup>c</sup> Untreated samples of II have been determined to be a 25:75 mixture of PA3AQ and PA3A(QH<sub>2</sub>), respectively.<sup>4</sup> <sup>d</sup> Oxidized with  $\text{PbO}_2$  to ~95% PA3AQ.

absorption broadening indicate that the various conformers existing in the ground state do not undergo appreciable interconversion during the lifetime of the excited singlet state ( $\leq 10 \text{ ns}$ ).

Fluorescence quantum yields of untreated II are lower than those of TTPa or PAPr (Table I). Since untreated II is ~75% in the hydroquinone form PA3A(QH<sub>2</sub>),<sup>4</sup> electron transfer can be ruled out as the principal mechanism of the strong quenching since the reduction potential of the hydroquinone moiety is presumably too negative.<sup>16</sup> We tentatively ascribe the observed fluorescence quenching in these systems to enhanced radiationless decay of the porphyrin excited singlet state within the intramolecular complexes that appear to exist between the hydroquinone and porphyrin moieties, as indicated by the absorption and emission spectra. Space-filling molecular models indicate that the structure of the linking bridge is sufficiently flexible to allow such complexes to form with at least one of the *meso*-position phenyl groups overlapping the  $\pi$ -electron system of the hydroquinone moiety. Molecular models of PA4A(DMB) indicate that the two methoxy groups present steric barriers such that intramolecular complexation would be less likely and hence the resulting perturbations of the  $\pi$ -orbitals of the porphyrin would be correspondingly weaker. This is consistent with the much weaker perturbations observed in the absorption and emission spectra for all of the dimethoxybenzene-linked porphyrins.

When II ( $n = 3$ ) is fully oxidized to PA3AQ, the fluorescence quantum yield drops to ~40% that of the corresponding untreated II, even when the excitation wavelength (~420 nm) favors the more strongly fluorescing species (see Table I). Clearly a new quenching mechanism is present in PA3AQ that is not present in PA3A(QH<sub>2</sub>). We interpret this additional quenching as being due to intramolecular electron transfer.

**c. Fluorescence Lifetimes.** Single-exponential fits were found to give satisfactory deconvolutions of the fluorescence decay profiles for TTPa and PAPr (Figure 3 and Table II). However, at least two exponential components were needed to obtain satisfactory fits of the decay curves for PA3A(DMB) and untreated II (Figure 3 and Table II). Note that for these latter two compounds the relative amplitudes of the respective short-lived components progressively increase when the excitation wavelength is changed from the blue edge of the Soret band (360 nm) to the maximum (420 nm) and then to the red edge (440 nm), either

(16) The measured reduction potentials (in  $\text{CH}_2\text{Cl}_2$ ) vs. SHE are 1.20 V for the radical cation of TTP<sup>17a</sup> and -0.35 V for methyl-*p*-benzoquinone.<sup>7,17b,c</sup> The lowest excited singlet state of TTP is ~1.89 V (656 nm; Figure 2a) above the ground state. Hence, light-induced electron transfer in the linked PA4AQ systems is estimated to be exergonic by about 0.34 eV (~33 kJ mol<sup>-1</sup>). "Hydroquinones do not exhibit anodic waves ... in the potential range of the reduction waves of the corresponding quinones".<sup>17b</sup> Also T. Shida of Kyoto University has shown that hydroquinone does not react with electrons produced by gamma irradiation of frozen mTHF.<sup>17d</sup>

(17) (a) Felton, R. H. In "The Porphyrins"; Dolphin, D., Ed.; Academic Press: New York, 1978; Part C, Vol. 5, p 66. (b) Mann, C. K.; Barnes, K. K. "Electrochemical Reactions in Nonaqueous Systems"; Marcel Dekker: New York, 1970; pp 190–195. (c) Zuman, P. "Substituent Effects in Organic Polarography"; Plenum Press: New York, 1967; pp 280–294. (d) T. Shida, personal communication.

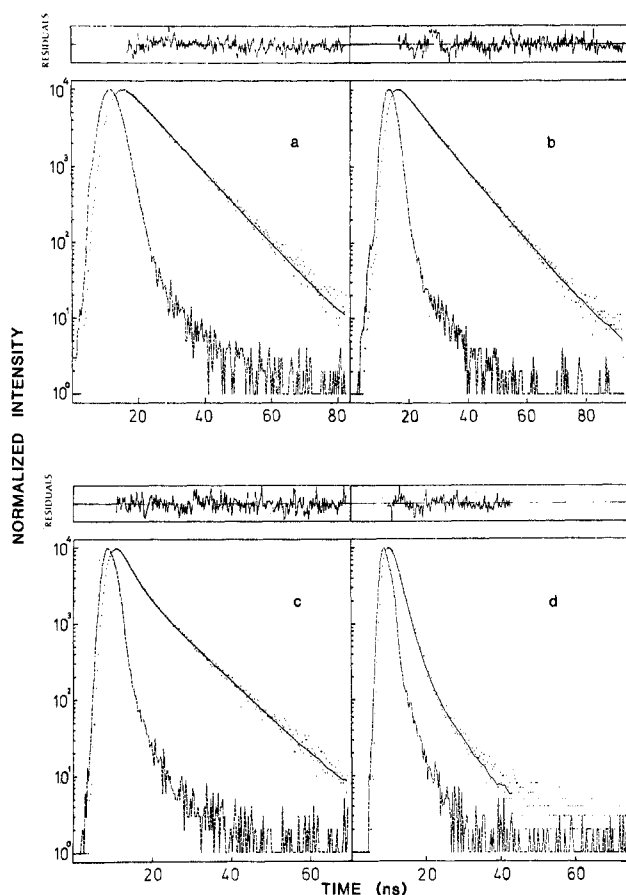


**Figure 3.** Fluorescence decay profiles obtained from  $\sim 10^{-6}$  M solutions at room temperature in  $\text{CH}_2\text{Cl}_2$  (excitation wavelength 420 nm, broad-band detection,  $\text{N}_2$  saturated). (a) PAPP. (b) PA3A(DMB). (c) II ( $n = 3$ ) (untreated). (d) II oxidized with  $\text{PbO}_2$  to PA3AQ. Analyses of these curves by computer deconvolution are presented in Tables II–IVa.

with broad-band ( $>640$  nm) or wavelength-selected detection. When PA3A(DMB) is excited at the blue edge of the Soret band (360 nm) and the emission is monitored at the maximum of the fluorescence spectrum (655 nm), a single long-lived component ( $\tau \sim 9$  ns) is observed. When both excitation and emission wavelengths are displaced to the red ( $\lambda_{\text{ex}} = 440$  nm,  $\lambda_{\text{em}} = 690$  nm; see Figures 1b and 2b) an enhanced contribution from the short-lived component is observed (Table II).

Untreated II ( $n = 3$ ) behaves in a similar manner as PA3A(DMB), except that the short-lived component is more pronounced in a two-component decay analysis. When  $\lambda_{\text{ex}} = 395$  nm and  $\lambda_{\text{em}} = 655$  nm, the short- and long-lived components have a ratio of  $\sim 2:1$ ; however, when both  $\lambda_{\text{ex}}$  and  $\lambda_{\text{em}}$  are shifted to the red (Table II), the amplitude ratio of the two components increases to  $\sim 6:1$ .

These results for PA3A(DMB) and untreated II ( $n = 3$ ), coupled with the absorption broadening in the Soret region and wavelength dependence of the fluorescence spectra and lifetimes, suggest the existence of at least two families of conformers<sup>18</sup> that do not appear to undergo appreciable interconversion during the lifetime of the lowest excited singlet state ( $\leq 10$  ns). We shall adopt a model in which one family of conformers is "extended",

(18) The existence of two distinct ground-state conformers has been observed in other similar systems: for example, anthryl-( $\text{CH}_2$ )<sub>3</sub>-dimethyl-aniline has been shown by Wang et al.<sup>19</sup> to exhibit such behavior. Also Van der Auweraer et al.<sup>20</sup> have found two kinetically distinct species for phenyl-( $\text{CH}_2$ )<sub>n</sub>-dimethyl-aniline, which they attribute to hindered rotation about the C–N bond. They note that: "Each conformation, as the word is used in this context, should be understood as an ensemble of several physical conformations in fast equilibrium with each other and both ensembles are separated by a relatively high energy barrier."

(19) Wang, Y.; Crawford, M. K.; Eisinger, K. B. *J. Phys. Chem.* **1980**, *84*, 2696–2698.

(20) Van der Auweraer, M.; Gilbert, A.; De Schryver, F. C. *J. Am. Chem. Soc.* **1980**, *102*, 4007–4017.

**Table II.** Analyses of the Fluorescence Decay Profiles for II ( $n = 3$ ) and Related Porphyrins in  $\text{CH}_2\text{Cl}_2$  at 295 K<sup>a</sup>

compd	$\lambda_{\text{ex}}$ , nm	$\lambda_{\text{em}}$ , nm	$A_S$ , %	$\tau_S$ , ns ( $\pm 0.1$ ), <sup>b</sup>	$A_L$ , %	$\tau_L$ , ns ( $\pm 0.1$ ), <sup>b</sup>	$\chi^2$
TTPa	420	$>640^c$			100	9.2	1.18
PAPr	420	$>640^c$			100	9.0	1.08
PA3A(DMB)	360	655 <sup>d</sup>			100	9.0	1.03 <sup>d</sup>
PA3A(DMB)	440	690 <sup>d</sup>	50	2.2	50	8.8	1.02 <sup>d</sup>
II ( $n = 3$ ) (untreated)	420	$>640^c$	73	2.7	27	8.7	1.04
II ( $n = 3$ ) (untreated)	440	$>640^c$	80	2.2	20	7.2	1.08
II ( $n = 3$ ) (untreated)	360	655 <sup>d</sup>	63	2.8	37	8.4	1.23 <sup>d</sup>
II ( $n = 3$ ) (untreated)	435	700 <sup>d</sup>	86	2.2	14	6.1	1.14 <sup>d</sup>
II ( $n = 3$ ) (oxidized)	360	655 <sup>d</sup>	89	1.9	11	7.4	1.13 <sup>d</sup>
II ( $n = 3$ ) (oxidized)	435	700 <sup>d</sup>	99.7	1.7	0.3	7.5	1.17 <sup>d</sup>

<sup>a</sup> The data were fit by computer deconvolution to a sum of two exponential components except for a few cases, such as TTPa and PAPr, where a single-exponential fit was found to be satisfactory. <sup>b</sup> Subscripts S and L refer to short and long lifetimes, respectively. The error quoted for lifetimes is the upper limit for any given run. <sup>c</sup> Broad-band detection with a Corning 2-58 cutoff filter. <sup>d</sup> Emission monochromator with near-IR gratings and a bandwidth of  $\sim 16$  nm. The total number of counts for these runs was about 5 times less than for the broad-band detection. Hence, the statistics for the  $\chi^2$  test are different. All the data in this set had  $\chi^2$  values within the acceptable range.

**Table III.** Double-Exponential Analyses of the Fluorescence Decay Profiles for Untreated and Oxidized II ( $n = 3$ )<sup>a</sup>

solvent	treatment	$A_S$ , %	$\tau_S$ , ns ( $\pm 0.1$ ), <sup>b</sup>	$A_L$ , %	$\tau_L$ , ns ( $\pm 0.1$ ), <sup>b</sup>	$\chi^2$
$\text{CH}_3\text{CN}$	untreated	76	3.6	24	11.5	1.15
$\text{CH}_3\text{CN}$	oxidized	97	2.6	3	8.9	1.55
$\text{CH}_2\text{Cl}_2$	untreated	73	2.7	27	8.7	1.04
$\text{CH}_2\text{Cl}_2$	oxidized	98	1.8	2	6.3	1.39
mTHF	untreated	69	3.5	31	11.6	1.18
mTHF	oxidized	92	2.7	8	7.3	1.75
diethyl ether	untreated	72	4.0	28	12.2	1.22
diethyl ether	oxidized	99	3.7	1	13.2 <sup>b</sup>	1.16

<sup>a</sup>  $\lambda_{\text{ex}} = 420$  nm,  $T = 295$  K, broad-band detection. <sup>b</sup>  $\pm 0.7$  ns.

giving rise to a single, unperturbed long-lived porphyrin emission ( $\tau_L$ ), and the other family of conformers is "complexed" such that the  $\pi$ -electron systems of the two moieties interact, leading to fluorescence quenching<sup>21</sup> and hence a shorter fluorescence lifetime ( $\tau_S$ ). As shown in Table II,  $\tau_S$  is shorter when the excitation wavelength is in the broadened red edge (440 nm) of the Soret band, indicating that those species which are interacting more

(21) Yamada et al.<sup>22</sup> have found that the Q-band absorption spectra of TTP in acetone, upon addition of benzoquinone, show evidence of a weak 1:1 complex between the porphyrin and quinone. Consistent with this finding, these systems exhibit static as well as dynamic quenching of the porphyrin fluorescence. Harriman and Hosie<sup>8f</sup> have found analogous quenching effects in the fluorescence lifetimes of symmetrically substituted *meso*-tetraphenylporphyrins (TPP). Thus the lifetimes of the tetrakis(*p*-methoxyphenyl)- and tetrakis(*p*-hydroxyphenyl)porphyrins are comparable to those of TPP and TTP ( $\sim 12$ – $15$  ns in outgassed benzene). However, the fluorescence is quenched in both tetra(*p*-quinolato)porphyrin ( $\sim 2.5$  ns) and its hydroquinone analogue, tetrakis(2,5-dihydroxyphenyl)porphyrin ( $\sim 7.5$  ns). In the former case, electron transfer has been invoked as the predominant quenching mechanism (see also ref 8a,d); whereas, in the latter case the enhanced electron-donating ability of the *meso* phenyl groups appears to be responsible for the diminished lifetime of the excited singlet state of the porphyrin.<sup>8f</sup> A similar effect may be responsible for the short fluorescence lifetimes that we observe for the complexed forms of PANAQH<sub>2</sub>.

(22) Yamada, S.; Sato, T.; Kano, K.; Ogawa, T. *Photochem. Photobiol.* **1983**, *37*, 257–262.

**Table IV.** Triple-Exponential Analyses of the Fluorescence Decay Profiles for Oxidized II ( $n = 3$ )

solvent	$A_1$ , %	$\tau_1$ , ns	$A_2$ , %	$\tau_2$ , ns	$A_3$ , %	$\tau_3$ , ns	$\chi^2$
a. Flashlamp Excitation, $\lambda_{\text{ex}} = 420$ nm; $T = 295$ K; Broad-Band Detection; Analysis Range 0–80 ns							
CH <sub>3</sub> CN	55 $1.9 \pm 0.2$		44 $3.3 \pm 0.3$	1	11.3 $\pm 0.7$	1.31	
CH <sub>2</sub> Cl <sub>2</sub>	88 $1.7 \pm 0.1$		11 $3.0 \pm 0.6$	1	8.4 $\pm 0.8$	1.29	
mTHI <sup>+</sup>	60 $2.1 \pm 0.1$		38 $4.1 \pm 0.3$	2	11.6 $\pm 0.9$	1.21	
diethyl ether	88 $3.4 \pm 0.1$		12 $5.7 \pm 0.3$	~0.2	25 $\pm 6$	1.13	
b. Laser Excitation, $\lambda_{\text{ex}} = 590$ nm; $T = 295$ K; Broad-Band Detection; Analysis Range 0–10 ns							
CH <sub>3</sub> CN	41 $0.14 \pm 0.02$	36	2.4 $\pm 0.1$	23	7.3 $\pm 0.2$	1.09	
CH <sub>2</sub> Cl <sub>2</sub>	8 $0.42 \pm 0.08$	76	1.9 $\pm 0.1$	16	6.0 $\pm 0.3$	1.10	

strongly are photoselected by the longer excitation wavelength. Hence, the shorter lifetime of each of the complexed conformers probably represents an average over a distribution of lifetimes reflecting different orientations and/or distances between the two moieties.

## 2. Time-Resolved Fluorescence Studies of Oxidized II ( $n = 3$ ).

Oxidation of the hydroquinone PA3A(QH<sub>2</sub>) to the corresponding quinone PA3AQ can be carried out efficiently by treatment with PbO<sub>2</sub>.<sup>4</sup> This treatment has no effect on the fluorescence properties of TTPa, PAPr, or PA3A(DMB) but strongly reduces the fluorescence yield and lifetimes of PA3A(QH<sub>2</sub>), the principal component of untreated II ( $n = 3$ ) (see Tables I and II). A similar strong decrease of fluorescence lifetimes is observed on oxidation of untreated II ( $n = 3$ ) to PA3AQ in other solvents (see Table III).

It is clear from Figure 3 and Tables II and III that oxidation of II with PbO<sub>2</sub> to >95% PA3AQ considerably diminishes the overall fluorescence lifetime and the amplitude of the long-lived component. Under conditions of photoselection (see last two entries in Table II), it appears that there are two components with lifetimes of ~1.7–1.9 and ~7.5 ns, respectively, with relative amplitudes that depend on the excitation and emission wavelengths. As in the case of PA3A(DMB) or untreated II ( $n = 3$ ), shifting  $\lambda_{\text{ex}}$  and  $\lambda_{\text{em}}$  to the red favors the short-lived component(s). However, attempts to achieve consistent results by deconvolution over various sample intervals of a given profile were not successful; for example, deconvolutions over the first 80 channels gave lifetimes considerably shorter than when the analyses were carried out over the last 80 channels. Thus, a two-exponential fit does not adequately describe the fluorescence decay. We therefore carried out three-exponential analyses (see Table IVa) which indicate that in each solvent the shorter-lived component obtained from a two-exponential deconvolution is itself comprised of at least two components. The longest lifetime  $\tau_3$  obtained from the three-component analysis is very close to  $\tau_L$  derived from the two-component analysis for the untreated samples of II. We assign this long-lived component  $\tau_3$  to a small proportion of the extended conformer that has not been oxidized by PbO<sub>2</sub>. Note that both  $\tau_1$  and  $\tau_2$  are longer in diethyl ether than in other more polar solvents; however, here the estimate of  $\tau_3$  is uncertain owing to its very small amplitude.

In order to check if any shorter-lived components are present in the PA3AQ emission, we conducted some preliminary experiments using a mode-locked dye laser at 590 nm as the excitation source. The resulting fluorescence decay profiles required at least three exponential components to obtain an acceptable fit; the results are summarized in Table IVb. Note that  $\tau_1$  is as short as ~140 ps in CH<sub>3</sub>CN and ~400 ps in CH<sub>2</sub>Cl<sub>2</sub> and that the set of lifetimes in Table IVb is different from the corresponding set in Table IVa. These findings indicate that purely statistical criteria for goodness of fit are not adequate to indicate the physical significance of the lifetime data obtained. We conclude that more than three fluorescent components are present; however, a further increase in the number of parameters to be fitted would lead to ambiguity and uncertainty. The physical meaning of the results from such an analysis would be questionable.

Clearly, there is a distribution of lifetimes probably corresponding to structural perturbations within the complexed and extended families of conformers. The laser experiments, which were analyzed over a much shorter time interval, would tend to emphasize shorter-lived components. The short values of  $\tau_1$  may still be instrument limited; however, by taking  $\tau_1$  from the laser experiments (Table IVb) and  $\tau_1$  from the flashlamp experiments (Table IVa), we can define an approximate range of lifetimes, which we assign to the complexed conformers. Similarly  $\tau_2$  from each set of experiments may define a range of lifetimes for the extended conformers, but the assignment is less clear in this case.

It appears from the preceding discussion that in PA3AQ we are observing a distribution of fluorescence lifetimes, which are associated with a range of electron-transfer rate constants, which, in turn, are associated with different specific geometries between donor and acceptor, especially within the complexed conformations. As a working hypothesis we ascribe  $\tau_1$  to the family of complexed conformers which are further quenched by electron transfer in the quinone form.<sup>23</sup> Within this model we can then obtain an expression for the apparent average electron-transfer rate constant in the complexed species as

$$k_1^{\text{et}} \cong \frac{1}{\tau_1} - \frac{1}{\tau_S} \quad (1)$$

where  $\tau_S$  represents the short lifetime of untreated II ( $n = 3$ ) from Table III (which is due predominantly to the complexed form of PA3A(QH<sub>2</sub>)).

In an analogous fashion we ascribe the longer lifetime  $\tau_2$  to fluorescence of the extended conformers of PA3AQ in which quenching by electron transfer also occurs.<sup>23</sup> The corresponding average rate constant in this case is given by

$$k_2^{\text{et}} \cong \frac{1}{\tau_2} - \frac{1}{\tau_L} \quad (2)$$

where  $\tau_L$  represents the longer-lived component in the fluorescence decay of untreated II ( $n = 3$ ), which we assume to arise predominantly from the extended conformers of PA3A(QH<sub>2</sub>). In each case, the quantum yield for electron transfer can be calculated from

$$\phi_i^{\text{et}} = k_i^{\text{et}} \tau_i \quad (3)$$

The electron-transfer rate constants and corresponding quantum yields are collected in Table V. The data for CH<sub>3</sub>CN and CH<sub>2</sub>Cl<sub>2</sub> include two sets of estimates of rate constants and quantum yields with the higher values being obtained from the laser-excitation experiments. The two values in each case can be interpreted as an estimate of the range of the distribution of electron-transfer rate constants within the two families of conformers. Note that the distribution of rate constants for the complexed set appears to be quite broad; this is understandable if we assume that the interaction in the complexed conformers is a strong function of the distance between and orientation of the porphyrin and quinone moieties. On the other hand, the distribution of rate constants for the extended family of conformers appears to be much narrower; again this would be expected if the interactions are weaker in these conformers.

It is apparent from Tables III and V that the dielectric constant (at least in moderately polar solvents) has little effect on the rate constants and quantum yields derived from the flashlamp-excitation experiments. The only significant effect occurs in diethyl ether.

**3. Temperature Dependence of Fluorescence Lifetimes.** Some experiments were carried out with flashlamp excitation and broad-band detection below room temperature down to ~140 K (see Figure 4). The data indicate that quenching brought about by the oxidation of untreated II ( $n = 3$ ) to PA3AQ diminishes

(23) The lifetimes obtained almost certainly represent a weighted average of lifetimes from a distribution of structures within each set of conformers. Estimates of  $k^{\text{et}}$  are based on the fluorescence lifetimes of the quinone form relative to the hydroquinone form of linked molecules and not relative to the unperturbed porphyrin; hence, the resulting weighted average values of  $k^{\text{et}}$  are probably close to lower limits.

Table V. Calculated Average Intramolecular Electron-Transfer Rate Constants and Quantum Yields for Oxidized II ( $n = 3$ )

solvent	dielectric constant	"complexed" conformers		"extended" conformers	
		$k_1^{\text{et}}$ $10^8 \text{ s}^{-1}$	$\phi_1^{\text{et}}$	$k_2^{\text{et}}$ $10^8 \text{ s}^{-1}$	$\phi_2^{\text{et}}$
CH <sub>3</sub> CN	37.5	$2.5 \pm 0.6$ $69 \pm 5^a$	$0.47 \pm 0.06$ $0.97 \pm 0.10^a$	$2.2 \pm 0.3$ $3.3 \pm 0.2^a$	$0.71 \pm 0.05$ $0.79 \pm 0.03^a$
CH <sub>2</sub> Cl <sub>2</sub>	9.1	$2.2 \pm 0.6$ $20 \pm 6^a$	$0.37 \pm 0.10$ $0.84 \pm 0.20^a$	$2.2 \pm 0.7$ $4.1 \pm 0.2^a$	$0.66 \pm 0.07$ $0.78 \pm 0.03^a$
mTHF	7.6	$1.9 \pm 0.2$	$0.40 \pm 0.03$	$1.6 \pm 0.2$	$0.65 \pm 0.03$
diethyl ether	4.3	$0.4 \pm 0.1$	$0.15 \pm 0.03$	$0.9 \pm 0.1$	$0.53 \pm 0.03$

<sup>a</sup> These data were calculated from the two shortest lifetimes obtained from the laser experiments (see Table IVb).

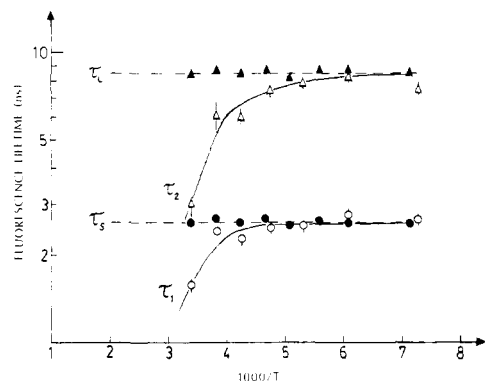


Figure 4. Temperature dependence of the fluorescence lifetimes of oxidized and untreated II ( $n = 3$ ) in CH<sub>2</sub>Cl<sub>2</sub> (N<sub>2</sub>-saturated) at an excitation wavelength of 420 nm and broad-band detection.  $\tau_1$  and  $\tau_2$  at each temperature were obtained from three-component deconvolutions of the fluorescence decay profiles for oxidized samples of II.  $\tau_S$  and  $\tau_L$  were derived from two-component fits of the corresponding decay profiles for untreated samples of II.

as the temperature is lowered; for temperatures below the freezing point of the solvent, there is no significant difference in lifetimes and amplitudes. Thus it appears that electron-transfer quenching is a thermally activated process, at least for data obtained from the flashlamp-excitation experiments.

Fluorescence lifetimes can be resolved to  $\sim 0.1$  ns; hence, from eq 1 and 2 we can place upper limits on possible low-temperature rate constants for  $k_1^{\text{et}}$  of  $k_2^{\text{et}}$  of  $\sim 1.5 \times 10^7$  to  $\sim 2 \times 10^6 \text{ s}^{-1}$ , respectively. The corresponding maximum quantum yields would be  $\sim 0.04$  and  $\sim 0.02$ , respectively. These quantum yields are in agreement with those found by EPR in paper 1.<sup>4</sup>

**4. Effect of Chain Length on the Fluorescence Properties of II ( $n = 2, 3, 4$ ).** The results of our analyses of the fluorescence decay curves for untreated and oxidized II ( $n = 2, 3$ , and 4) are collected in Table VI. The extent of oxidation with PbO<sub>2</sub> (as determined from UV-absorption measurements<sup>4</sup>) is about 75% for  $n = 2$  and 4 and  $>95\%$  for  $n = 3$ . Only in the case of  $n = 3$  are the relative amplitudes of the short- and long-lived components markedly affected by the oxidation treatment. For  $n = 2$  and 4 the amplitudes change in the same direction on oxidation as for  $n = 3$ , but the effect is much smaller. Since multiphasic decay is observed for all values of  $n$ , we conclude that both the extended and complexed conformers are present in all three homologues. However, the relative amplitude data in Table VI suggest that the complexed conformers dominate in  $n = 2$  and 3, whereas the extended conformers dominate in  $n = 4$ . This conclusion is also supported by the fact that the Soret bands in the absorption spectra are more strongly perturbed for  $n = 2$  and 3 than for  $n = 4$  (see Figure 1c).

Our data indicate that the methylene chain with  $n = 3$  is the optimum length for electron-transfer quenching of the porphyrin excited singlet state. With  $n = 2$  the chain may be too short to fold easily into the structure(s) required for rapid electron transfer, whereas, the chain with  $n = 4$  may introduce so many new conformational possibilities that the molecule has a low average probability of being in the optimum configuration(s) for electron transfer.

Table VI. Double-Exponential Analyses of Fluorescence Decay Profiles for Untreated and Oxidized II ( $n = 2, 3$ , and 4) in CH<sub>2</sub>Cl<sub>2</sub><sup>b</sup>

compd	$A_S$ , %	$\tau_S$ ( $\pm 0.1$ ), ns	$A_L$ , %	$\tau_L$ ( $\pm 0.1$ ), ns	$\chi^2$
II ( $n = 2$ ) (untreated)	68	3.2	32	8.8	1.19
II ( $n = 2$ ) (oxidized)	74	3.2	26	8.7	1.25
II ( $n = 3$ ) (untreated)	73	2.7	27	8.7	1.04
II ( $n = 3$ ) (oxidized)	98	1.8	2	6.3	1.39
II ( $n = 4$ ) (untreated)	12	3.7	88	9.7	1.27
II ( $n = 4$ ) (oxidized)	30	3.1	70	9.2	1.27

<sup>a</sup> Triple-exponential analyses of oxidized II ( $n = 2$  or 4) were not carried out because of the small changes observed on oxidation. <sup>b</sup>  $\lambda_{\text{ex}} = 420$  nm,  $T = 295$  K, broad-band detection.

## Conclusions

Our time-resolved fluorescence data of the linked porphyrin-quinone molecules are interpreted in terms of a quenching mechanism that involves electron transfer from the lowest excited singlet state of the porphyrin to the attached quinone in the same molecule. Absorption and fluorescence data indicate that these linked molecules exist in two more or less distinct families of conformers in both the ground and excited states. One set of conformers (complexed) appears to be folded so that the porphyrin and quinone are sufficiently close that their  $\pi$ -electron systems interact, while in the other set of conformers (extended) the porphyrin and quinone do not appear to interact significantly. Both sets of conformers of PA3AQ appear to undergo rapid ( $>10^8 \text{ s}^{-1}$ ) photoinduced electron transfer in polar or moderately polar solvents with a range of rate constants spanning a factor of  $\geq 40$ . Thus, close proximity of the porphyrin and quinone moieties does not seem to be the only geometric requirement for fast light-induced electron transfer.

We note from Table V that for the flashlamp-excitation experiments,  $k^{\text{et}}$  for the two families of conformers is about the same ( $\sim 2 \times 10^8 \text{ s}^{-1}$ ) in moderately polar solvents. However, in the laser-excitation experiments,  $k^{\text{et}}$  was found to be much faster for the complexed as compared to the extended conformers. As noted before, the data from the laser-excitation experiments emphasizes the shorter-lived components, which probably arise from more tightly complexed conformers. It is perhaps anomalous that larger differences are not found in  $k^{\text{et}}$  for the two families of conformers. Miller and co-workers<sup>24</sup> have found that electron transfer between unlinked donors and acceptors exhibits an exponential dependence on distance. In our case electron transfer can take place, either through space (i.e., through the solvent matrix as in Miller's experiments) or along the linking chain. The former mechanism should be strongly dependent on the distance between the porphyrin and quinone moieties and may be operative in some of the more tightly bound complexed conformers. However, electron transfer may involve interactions through the linking chain; this mechanism would be less sensitive to geometrical factors between the donor and acceptor moieties.

The data obtained at low temperatures suggest that electron transfer along the linking chain is probably strongly dependent<sup>25</sup>

(24) (a) Beitz, J. V.; Miller, J. R. *J. Chem. Phys.* **1979**, *71*, 4579-4595. (b) Miller, J. R.; Beitz, J. V. *J. Chem. Phys.* **1981**, *74*, 6746-6756.

on specific bond-to-bond overlap at each link in the chain. At room temperature, bond rotations (particularly in the methylene chain) will be rapid, and optimum overlap conditions can be achieved within the lifetime of the excited singlet state. However, at low temperatures such optimum orientations of the chain will exist for only a small proportion of the PQ molecules, and these may be the ones responsible for the observed EPR signals.<sup>4</sup>

The behavior of the "complexed" PA3AQ conformers shares some common features with certain classes of bichromophoric molecules with a donor and acceptor linked directly.<sup>26</sup> In these nonporphyrinic molecules excited-state electron transfer takes place only after the two chromophores rotate to a mutually perpendicular conformation, thus minimizing their  $\pi$ -electron overlap. The temperature dependence of  $k^{\text{et}}$  for both sets of conformers indicates the importance of such dynamic reorientation factors. However, too little is known about the geometry and conformational mobility of the porphyrin-quinone molecules studied to date to draw any firm conclusions about orbital rules for electron transfer. This would require the study of a series of molecules with rigid linkages and fixed orientations between the donor and acceptor.

Our data show that solvent polarity is not the dominating influence on the average values of the electron-transfer rate constants, at least for solvents with dielectric constants in the range of 6–37. In a less polar medium such as diethyl ether ( $\epsilon = 4.3$ ), the apparent electron-transfer rate constants are much lower, especially in the case of the complexed conformers. Hence, there appears to be a "dielectric threshold" above which the rate of electron transfer is not strongly dependent on polarity but below which the rate constant is markedly lower. Mataga and co-workers<sup>27</sup> have demonstrated that polar solvents strongly enhance the light-induced formation of intramolecular exciplexes involving an electron-transfer process in a series of aryl-(CH<sub>2</sub>)<sub>n</sub>-N,N-dialkylaniline derivatives ([Ar-(CH<sub>2</sub>)<sub>n</sub>-DAA]). These workers concluded that such exciplexes are "loose" in polar solvents but "tight" in nonpolar solvents, leading to more rigorous structural requirements for electron transfer in the latter case.

The fluorescence data for PANAQ as a function of the length of the methylene bridge indicate an apparent optimum at  $n = 3$

for the electron-transfer process. This is consistent with the low-temperature EPR studies of these compounds,<sup>4</sup> in which the quantum yield for net electron transfer is higher for  $n = 3$  and  $n = 2$  molecules than for  $n = 4$  molecules. This same feature has been observed for the Ar-(CH<sub>2</sub>)<sub>n</sub>-DAA series<sup>27</sup> discussed above and for a series of homologous naphthyl-(CH<sub>2</sub>)<sub>n</sub>-dimethylamine derivatives.<sup>28</sup> The so-called " $n = 3$  rule" has also been observed for excimer formation in Ar-(CH<sub>2</sub>)<sub>n</sub>-Ar compounds,<sup>29</sup> for which the structural requirements appear to be more rigorous than for the heteroexcimers studied by Mataga and co-workers.<sup>27</sup> This suggests that the -(CH<sub>2</sub>)<sub>3</sub>- chain represents the best compromise between having the donor and acceptor sufficiently close for electron transfer and yet flexible enough for the molecules to achieve an optimum orientation during the lifetime of the excited singlet state.

It is clear from the results presented here and in paper 1<sup>4</sup> that the most important geometric factor affecting the rate of electron-transfer in these linked porphyrin-quinone molecules is the ability of the two moieties to assume an optimum configuration. We draw the same conclusion from nanosecond laser flash photolysis studies of these linked molecules, the details of which will be presented in a future paper in this series.<sup>30</sup>

Results obtained to date on these flexibly linked PQ molecules are encouraging in that some qualitative features of the effects of molecular geometry are beginning to emerge. It is probable, however, that elucidation of the precise details of the geometric requirements for efficient photochemical electron transfer and subsequent charge stabilization can be obtained only from studies of rigidly linked molecules in which the donor and acceptor have known orientations and spacings with respect to each other. Such studies are currently in progress in these laboratories.

**Acknowledgment.** We thank E. Templeton, Prof. R. K. Bauer, Dr. K. L. Marsh, and D. R. Cook for their assistance in the fluorescence-lifetime measurements and Prof. W. R. Ware for the use of his fluorescence laboratory. We also thank Prof. S. J. Strickler of the University of Colorado at Boulder for valuable discussions. We are grateful to the Richard and Jean Ivey Foundation for a generous grant which allowed UWO to purchase the fluorescence-lifetime apparatus.

Work at UWO was supported by a Strategic Grant in Energy to J.R.B. and A.C.W. and an Operating Grant to M.J.S. from the Natural Sciences and Engineering Research Council of Canada and by an Academic Development Fund Equipment Grant to M.J.S. from The University of Western Ontario. Work at SERI was supported by the Division of Chemical Sciences, Office of Basic Energy Sciences, U.S. Department of Energy, under Contract EG-77-C-01-4042.

**Registry No.** TTPa, 61449-63-6; PAPr, 87586-69-4; PA3A(DMB), 87586-70-7; PA3A(QH<sub>2</sub>), 87586-71-8; PA3AQ, 84445-21-6; PA2A(QH<sub>2</sub>), 87586-72-9; PA4A(QH<sub>2</sub>), 87586-73-0.

(25) Larsson, S. J. *J. Am. Chem. Soc.* **1981**, *103*, 4034–4040.

(26) (a) Grabowski, Z. R.; Rotkiewicz, K.; Siemiarczuk, A.; Cowley, J. C.; Baumann, W. *Nouv. J. Chim.* **1979**, *3*, 443–454. (b) Rotkiewicz, K.; Grellmann, K. H.; Grabowski, Z. R. *Chem. Phys. Lett.* **1973**, *19*, 315–318. (c) Rotkiewicz, K.; Grabowski, Z. R.; Krowczynski, A.; Kühnle, W. *J. Lumin.* **1976**, *12/13*, 877–885. (d) Rotkiewicz, K.; Grabowski, Z. R.; Jasny, J. *Chem. Phys. Lett.* **1975**, *34*, 55–59. (e) Siemiarczuk, A.; Grabowski, Z. R.; Krowczynski, A.; Asher, M.; Ottolenghi, M. *Chem. Phys. Lett.* **1977**, *51*, 315–320. (f) Grabowski, Z. R.; Rotkiewicz, K.; Siemiarczuk, A. *J. Lumin.* **1979**, *18/19*, 420–424. (g) Rettig, W.; Bonacic-Koutecky, V. *Chem. Phys. Lett.* **1979**, *62*, 115–120. (h) Siemiarczuk, A.; Koput, J.; Pohorille, A. *Z. Naturforsch. A* **1982**, *37A*, 598–606. (i) Klein, U. A.; Hafner, F. W. *Chem. Phys. Lett.* **1976**, *43*, 141–145.

(27) (a) Migita, M.; Ada, T.; Mataga, N.; Nakashima, N.; Yoshihara, K.; Sakata, Y.; Misumi, S. *Chem. Phys. Lett.* **1980**, *72*, 229–232. (b) Mataga, N.; Migita, M.; Nishimura, T. *J. Mol. Struct.* **1978**, *47*, 199–219. (c) Migita, M.; Kawai, M.; Mataga, N.; Sakata, Y.; Misumi, S. *Chem. Phys. Lett.* **1978**, *53*, 67–70. (d) Mataga, N.; Okada, T.; Masuhara, H.; Nakashima, N.; Sakata, Y.; Misumi, S. *J. Lumin.* **1976**, *12/13*, 159–168. (e) Okada, T.; Fujita, T.; Kubota, M.; Mataga, N.; Ide, R.; Sakata, Y.; Misumi, S. *Chem. Phys. Lett.* **1972**, *14*, 563–568.

(28) Chandross, E. A.; Thomas, H. T. *Chem. Phys. Lett.* **1971**, *6*, 393–396.

(29) (a) Hirayama, F. *J. Chem. Phys.* **1965**, *42*, 3163–3171. (b) Chandross, E. A.; Dempster, C. J. *J. Am. Chem. Soc.* **1970**, *92*, 3586–3593.

(30) Connolly, J. S.; Bolton, J. R.; Marsh, K. L.; Cook, D. R.; Ho, T.-F.; Weedon, A. C., paper 3 of this series, to be submitted for publication.